

# Synthesis and Sensing Properties of ZnO/ZnS Nanocages

Xue-Lian Yu · Hui-Ming Ji · Hong-Li Wang ·  
Jing Sun · Xi-Wen Du

Received: 30 October 2009 / Accepted: 5 January 2010 / Published online: 16 January 2010  
© The Author(s) 2010. This article is published with open access at Springerlink.com

**Abstract** Large-scale uniform ZnO dumbbells and ZnO/ZnS hollow nanocages were successfully synthesized via a facile hydrothermal route combined with subsequent etching treatment. The nanocages were formed through preferential dissolution of the twinned (0001) plane of ZnO dumbbells. Due to their special morphology, the hollow nanocages show better sensing properties to ethanol than ZnO dumbbells. The gain in sensitivity is attributed to both the interface between ZnO and ZnS heterostructure and their hollow architecture that promotes analyte diffusion and increases the available active surface area.

**Keywords** ZnO/ZnS · Hollow · Nanocages · Ethanol sensing · Interface

## Introduction

Nanomaterials with hollow appearance are drawing intense research interest because these structures often exhibit interesting properties that are different from those of

particles, thus making them attractive from both scientific and technological viewpoints. The fabrication of hollow structures with homogenous shells will open up possibilities for various application fields, such as controlled-release capsules, artificial cells for drug delivery, lightweight fillers, shape-selective adsorbents, and catalysts [1]. Several methodologies have been developed to achieve these special nanostructures, for example galvanic-replacement reactions have been successfully used to produce Au nanoboxes [2], nanocages [3]; single-crystalline Pd nanoboxes, and nanocages were obtained by a surface metal-corrosion process [4], and Co cubic nanoskeletons have been synthesized by a simple one-pot solution method [5]. Furthermore, hetero-nanostructures with hollow appearance have attracted considerable attention nowadays because of their amazingly complicated structures as well as their outstanding properties and broad potential applications [6–8]. A number of remarkable features of these materials include huge specific area, flexible chemical compositions, and multiphase anisotropic interfaces [9]. Most of these properties are desired pursuits of scientists.

As important wide band gap semiconductors, ZnO and ZnS have a wide range of applications for optical and electric devices. And the studies of ZnO/ZnS heterostructures with various morphologies, such as nanorings [10], biaxial nanowires [11], and saw-like nanostructures [12], have been reported. However, the synthesis of ZnO/ZnS heterojunction hollow nanocages still remains a challenge. In this work, a template-free hydrothermal route combined with subsequent etching treatment is demonstrated for the synthesis of ZnO/ZnS hollow nanocages. A comparative gas-sensing study between the as-prepared ZnO dumbbells and ZnO/ZnS hollow nanocages was performed to depict the superior sensing properties of these hollow hetero-nanocages.

---

X.-L. Yu · H.-M. Ji · J. Sun · X.-W. Du (✉)  
School of Materials Science and Engineering, Tianjin  
University, 300072 Tianjin, People's Republic of China  
e-mail: xwdu@tju.edu.cn

X.-L. Yu  
Motorola (China) Electronics Ltd, No. 10, 4th Avenue, TEDA,  
300457 Tianjin, People's Republic of China

H.-L. Wang  
School of Mechanical Engineering, Tianjin University,  
300072 Tianjin, People's Republic of China

## Experimental

### Preparation of ZnO Dumbbell Nanostructure

In a typical preparation process, the hexamethylenetetramine (HMT) aqueous solution ( $10 \text{ mmol L}^{-1}$ ) was mixed with zinc nitrate ( $\text{Zn}(\text{NO}_3)_2$ ) aqueous solution ( $10 \text{ mmol L}^{-1}$ ) under vigorous magnetic stirring at  $90^\circ\text{C}$  for 3 h and then cooled to room temperature naturally. The resultant white solid product was centrifuged, washed with distilled water and alcohol in turns, and then dried in vacuum at  $60^\circ\text{C}$  for 6 h.

### Preparation of ZnO/ZnS Hollow Nanocages

To convert ZnO to ZnO/ZnS hetero-nanostructure, thioacetamide ( $\text{CH}_3\text{CSNH}_2$ ) was used to supply sulfide ions.  $\text{CH}_3\text{CSNH}_2$  aqueous solution (4 mM) was added into 50 mL as-prepared ZnO suspension. Then, the mixture solution was heated under stirring on a hot plate at  $90^\circ\text{C}$  for 3 h. After the reaction, the obtained ZnO/ZnS precipitates were separated by centrifugation, washed with deionized water, and dried at  $60^\circ\text{C}$  for 2 h.

### Characterization

The X-ray diffractometry (XRD) for the crystal structure of the products was carried out in a Rigaku D/max 2500v pc diffractometer. The morphology of samples was observed using a Hitachi S-4800 field-emission scanning electron microscope (FESEM) and a FEI Tecnai G2 F20 transmission electron microscope (TEM) with a field-emission gun operating at 200 kV. Photoluminescence (PL) analyses with a Hitachi F-4500 fluorescence spectrometer were performed on aqueous solutions directly at room temperature using 325 nm as the excitation wavelength. The gas-sensitive properties were measured using a static test system (Hanwei Electronics, China).

## Results and Discussion

X-ray diffraction was used to confirm the crystal structure of the hetero-nanostructure. As shown in Fig. 1, after the reaction of ZnO nanoparticles with  $\text{CH}_3\text{CSNH}_2$ , the hetero-structured composites were formed. In addition to hexagonal structure ZnO (JCPDS 79-2205), new peaks located at  $2\theta$  values of  $29.1^\circ$  and  $48.4^\circ$  appear, which can be indexed to the cubic ZnS (JCPDS 79-0043). Such a result demonstrates that the  $\text{CH}_3\text{CSNH}_2$  treatment leads to the formation of ZnS by partially sulfurizing ZnO nanoparticles.

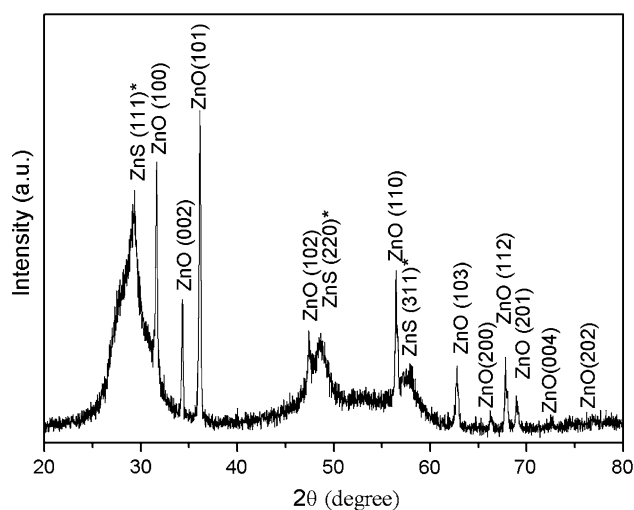


**Fig. 1** XRD pattern of the synthesized ZnO/ZnS hetero-nanostructure

The morphologies of the nanostructures before and after sulfurization are shown in Fig. 2. The ZnO template with dumbbell shape consists of two hexagonal ZnO crystals with length of about  $1 \mu\text{m}$  and diameters of 400 nm (Fig. 2a). After sulfurization, the shape of ZnO template is retained, but the inner structure becomes hollow, defined as nanocage (as shown in Fig. 2b). Furthermore, we can see both the dumbbell-like and cage-like products have boundaries in the middle. TEM image of dumbbell-like ZnO template is shown in Fig. 2c, which agrees well with the SEM results. The high-resolution TEM (HRTEM) image (Fig. 2d) indicates the dumbbell-like ZnO is of high crystallinity and [0001] direction oriented. Figure 2e is the TEM image of as-prepared ZnO/ZnS nanocage structure. The strong contrast between the dark edge and the pale center is indicative of the hollow nature of the cage. It is clearly seen that the nanocage has a shell thickness of about 30 nm. The HRTEM image (Fig. 2f) taken from the edge of the nanocage shows the existence of ZnS nanocrystals, which form a thin layer of about 5 nm. The HRTEM image further confirms that the hollow nanocage is a hetero-structure composed of ZnO and ZnS.

The growth mechanism of ZnO dumbbells and ZnO/ZnS hollow nanocages are illustrated in Fig. 3. For the dumbbell structure, it is mainly related to the hexagonal ZnO crystal structure, which has both polar and nonpolar faces. As the literature reported [13–15], during the reaction, the growth units,  $\text{ZnO}_2^{2-}$  and  $(\text{CH}_2)_6\text{N}_4\text{--}4\text{H}^+$ , adsorb on the different polar faces of the crystal surface, resulting in faster growth along the [0001] and [000-1] directions simultaneously, which is significantly different from the usual [0001] growth occurred in the formation of ZnO single crystal.

ZnO can react with sulfide ions released from  $\text{CH}_3\text{CSNH}_2$  and convert into ZnS via the following reactions:

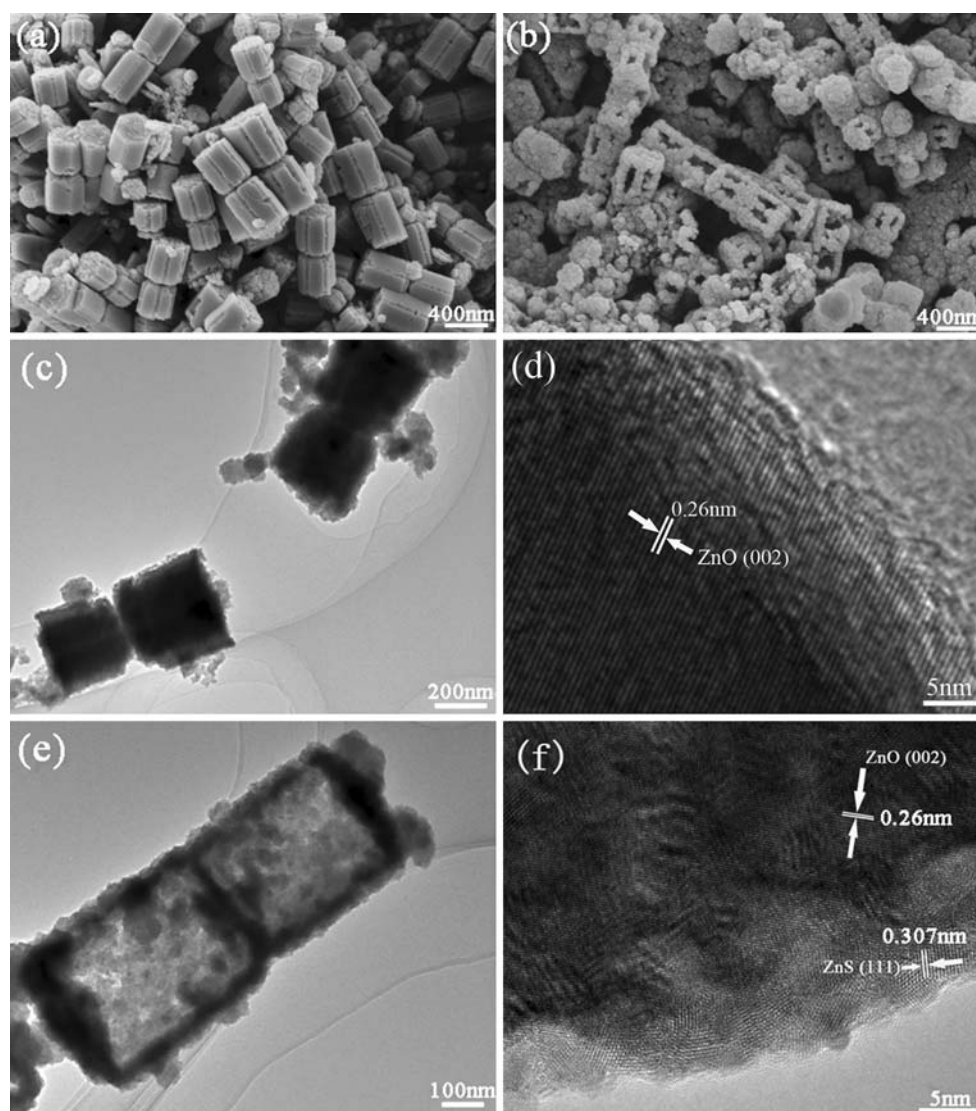


**Fig. 2** SEM images of ZnO dumbbells (a) and ZnO/ZnS hollow nanocages (b); TEM and HRTEM images of ZnO dumbbells (c, d) and ZnO/ZnS hollow nanocages (e, f)

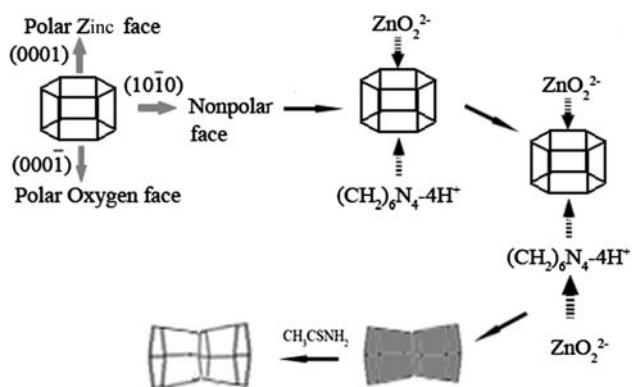
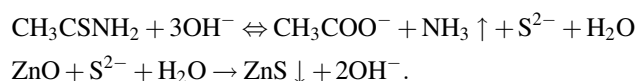


**Fig. 3** Illustration of the growth mechanism of ZnO dumbbells and ZnO/ZnS nanocages



Such reactions can proceed preferentially at the end planes and ridges of the ZnO prism, where many defects were observed in SEM and TEM images, as a result, ZnS nanocrystals can be formed at those sites and connect into a frame; the further growth of ZnS nanocrystals would consume ZnO at the planar surface and the inner of the dumbbells, which results in nanocages with ZnS shell and regular interior space.

Figure 4 shows the room temperature PL spectra of the ZnO/ZnS hollow nanocages with different reaction time as well as the ZnO dumbbells. Except for the noise signals

from the instrument (450 and 460 nm), the typical PL spectra of ZnO/ZnS hetero-nanocages exhibit three ultraviolet emission bands centered at  $\sim 360$ , 384, and 398 nm. According to the pure ZnO dumbbell nanostructure, the strong UV emission at 398 nm may originate from the excitonic recombination corresponding to the near band edge emission of ZnO [16], while the newly arisen peak

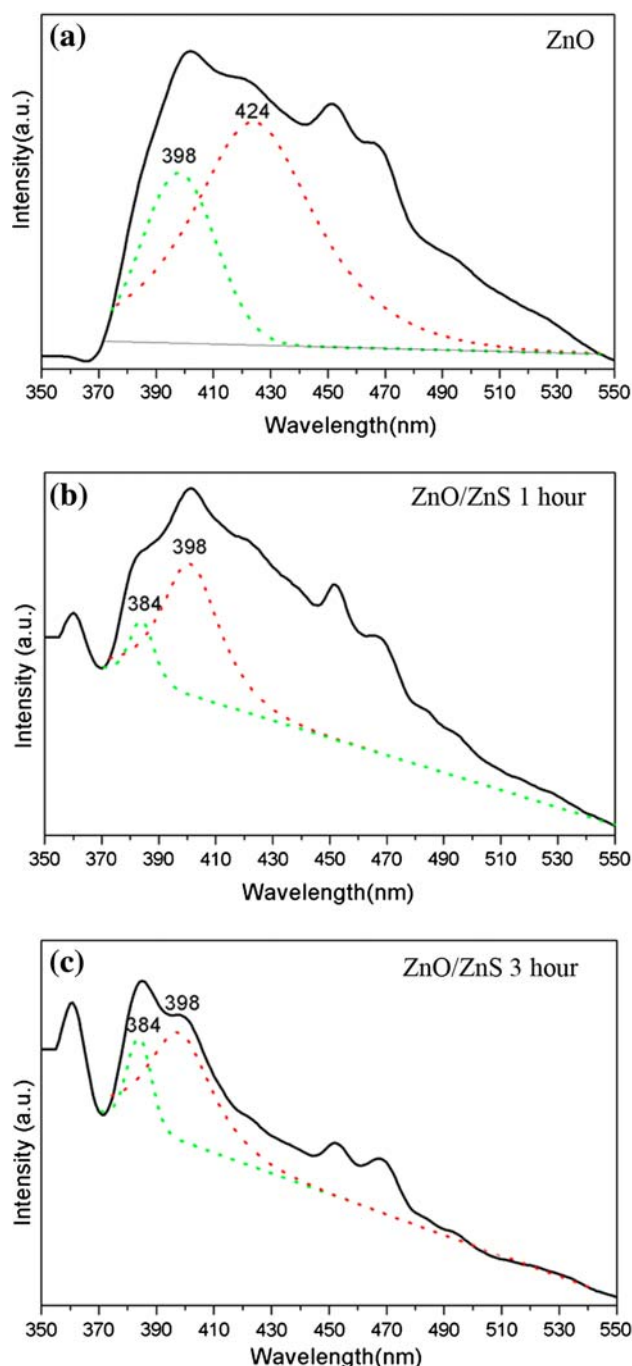


**Fig. 4** PL spectra of ZnO dumbbells and ZnO/ZnS hollow nanocages with different reaction times. **a** Pure ZnO, **b** after 1-h sulfuration, **c** after 3-h sulfuration

centered at 360 nm should be ascribed to the formation of ZnS nanocrystals. As sulfurization goes on, the relative intensity of the peaks centered at 360 and 398 nm changes, which indicates more ZnO transformed to ZnS nanocrystals. Besides, a new ultraviolet emission peak ( $\sim 384$  nm) is found in products both 1- and 3-h sulfuration. It has been proven by using band-corrected pseudopotential density functional theory that the ZnO/ZnS hetero-nanostructure can induce new interface state and related photoluminescence [17]. According to the structure characterization and growth mechanism analysis, this ultraviolet emission peak ( $\sim 384$  nm) could be assigned to the interface between ZnO and ZnS structure. The gradually enhanced intensity of the PL peaks related to ZnS and the interface suggests that the total amounts of ZnS nanocrystals and the ZnO/ZnS interface increase with the reaction time.

Prompted by the hollow appearance of the as-prepared ZnO/ZnS nanocages, we suspect that these nanostructures could be useful in fabricating gas sensors. For comparison, we made sensors using the ZnO dumbbells and ZnO/ZnS nanocages, respectively. The schematic diagram of sensor is shown in Fig. 5a. Nanocage powders were coated on a ceramic tube with two golden electrodes at each end. The powders on ceramic tube were then sintered at 300°C, afterward, electrical contacts were made by attaching two

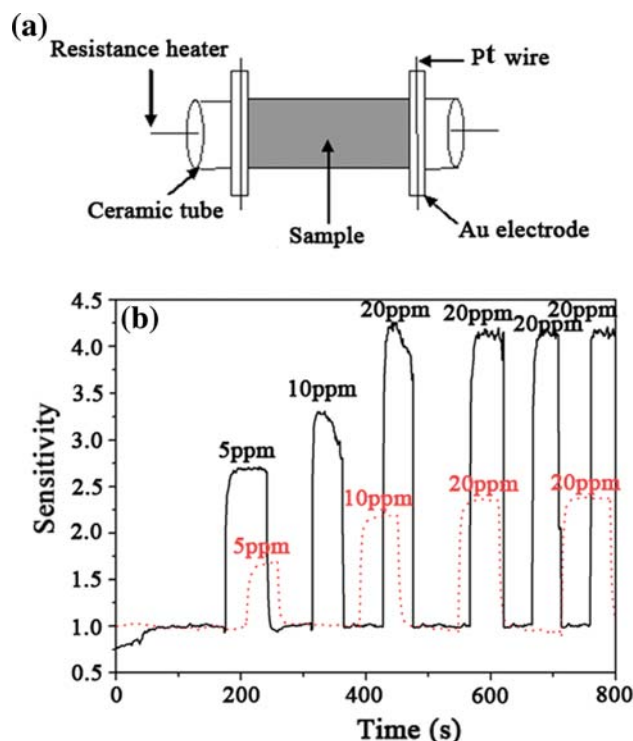


**Fig. 5** **a** Schematic representation of a typical gas sensor, **b** response curves of ZnO dumbbells (red) and ZnO/ZnS hollow nanocages (black) to ethanol with increasing concentrations at 210°C

platinum wires with the electrodes. Gas-sensing measurements were made in a static system and the test gas was introduced into the testing chamber by injection. As can be seen from Fig. 5b, the sensor made of ZnO/ZnS hollow nanocages exhibits gradual increase in sensitivity ( $R_{\text{air}}/R_{\text{gas}}$ , where  $R_{\text{air}}$  is the resistance in atmospheric air and  $R_{\text{gas}}$  is the resistance of the sensor in a special gas) with an increase in ethanol gas concentration. The sensitivity reaches 4.2 for 20 ppm ethanol, which is much higher than that made of ZnO dumbbells (2.3). According to Fig. 5b, the response time of the ZnO dumbbell and ZnO/ZnS hetero-structure nanocages sensors is about 15s and 5s to alcohol, respectively.

The enhanced sensitivity of the ZnO/ZnS hollow nanocages sensor to ethanol gas is attributed to both the unique morphology and the heterojunction between ZnO and ZnS. Theoretically, the rate of the surface reaction is in proportion to the number of available adsorption sites on the outer surface of nanostructure [18]. This illustrates that the loose and porous structure is clearly more favorable for the diffusion of gas molecules than the compact structure of nanoparticles. Thus, the hollow morphology endows the ZnO/ZnS nanocages strong capability to absorb and desorb gas molecules, and then contributes to the excellent sensing properties. Apart from this, the heterojunction structure between ZnO and ZnS also plays an important role in improving the sensing properties. According to the space-charge layer mode [19], as the sensor is exposed to air, oxygen molecules will be adsorbed on the oxide surface, and extract electrons in the bulk, leading to a narrow conduction channel. In contrast, when the sensor is exposed to reducing gases, the trapped electrons will be released owing to reactions between reducing gases and adsorbed oxygen molecules, and then the conduction channel changes wider. In ZnO/ZnS heterostructure, oxygen molecules in air should deplete electrons in both ZnS shell and ZnO core [20]. On the other hand, electrons may be scattered by the interface between ZnO and ZnS, which has been proved existence according to the PL spectrum in Fig. 4. The above two factors jointly cause a higher electric resistance of ZnO/ZnS heterostructure in air. As exposed to ethanol vapor, the ethanol reacts with the adsorbed oxygen species, and the extracted electrons from both ZnO core and ZnS shell can be released, resulting in an improved sensitivity of the ZnO/ZnS heterostructure compared with that of bare ZnO.

## Conclusion

In summary, based on a hydrothermal route combined with subsequent etching process, ZnO dumbbells and ZnO/ZnS

hollow nanocages were synthesized at a large scale. The photoluminescence and gas-sensing properties of these structures were studied. Due to their special morphology, the ZnO/ZnS hollow nanocages show excellent sensing properties to ethanol, including high sensitivity, rapid response rate, and fast recovery. Apparently, the gain in sensitivity is attributed to both the hollow architecture and the heterojunction between ZnO and ZnS nanostructure. Therefore, the prepared ZnO/ZnS hollow nanocages can be used as an efficient sensor for detecting ethanol with fast response and good reproducibility.

**Acknowledgments** This work was supported by the Natural Science Foundation of China (No. 10732020 and No. 50672065), National High-tech R&D Program of China (No. 2007AA021808 and 2009AA03Z301) and the National Science Foundation for Post-doctoral Scientists of China (20090450089).

**Open Access** This article is distributed under the terms of the Creative Commons Attribution Noncommercial License which permits any noncommercial use, distribution, and reproduction in any medium, provided the original author(s) and source are credited.

## References

1. J.N. Cha, H. Birkedal, L.E. Euliss, M.H. Bart, M.S. Wong, T.J. Deming, G.D. Stucky, *J. Am. Chem. Soc.* **125**, 8285 (2003)
2. Y. Sun, B.T. Mayers, Y. Xia, *Nano. Lett.* **2**, 481 (2002)
3. J. Chen, D. Wang, J. Xi, L. Au, A.R. Siekkinen, A. Warsen, Z.Y. Li, H. Zhang, Y. Xia, X. Li, *Nano. Lett.* **7**, 1318 (2007)
4. Y. Xiong, J. Chen, Z.Y. Li, Y. Yin, Y. Xia, *Angew. Chem. Int. Ed.* **44**, 7913 (2005)
5. X. Wang, H.B. Fu, A.D. Peng, T.Y. Zhai, Y. Ma, F.L. Yuan, J.N. Yao, *Adv. Mater.* **21**, 1636 (2009)
6. B. Liu, H.C. Zeng, *Small* **1**, 566 (2005)
7. X.W. Lou, C.L. Yuan, L.A. Archer, *Adv. Mater.* **19**, 3328 (2007)
8. J. Li, H.C. Zeng, *J. Am. Chem. Soc.* **129**, 15839 (2007)
9. Y. Zhao, L. Jiang, *Adv. Mater.* **21**, 3621 (2009)
10. X. Wu, P. Jiang, Y. Ding, W. Cai, S.S. Xie, Z.L. Wang, *Adv. Mater.* **19**, 2319 (2007)
11. J. Yan, X. Fang, L. Zhang, Y. Bando, U.K. Gautam, B. Dierre, T. Sekiguchi, D. Golberg, *Nano. Lett.* **8**, 2794 (2008)
12. G. Shen, D. Chen, C.J. Lee, *J. Chem. Phys. B* **110**, 15689 (2006)
13. K. Govender, D.S. Boyle, P.B. Kenway, *J. Mater. Chem.* **14**, 2575 (2004)
14. Q.J. Yu, C.L. Yu, H.B. Yang, W.Y. Fu, L.X. Chang, J. Xu, C.L. Shao, Y.L. Liu, *Inorg. Chem.* **46**, 6204 (2007)
15. A. Wei, X.W. Sun, C.X. Xu, Z.L. Dong, Y. Yang, S.T. Tan, W. Huang, *Nanotechnology* **17**, 1740 (2006)
16. F. Li, Y. Jiang, L. Hu, L.Y. Liu, Z. Li, X.T. Huang, *J. Alloys Compd.* **474**, 531 (2009)
17. J. Schrier, D.O. Demchenko, L. Wang, *Nano. Lett.* **7**, 2377 (2007)
18. J. Zhang, S.R. Wang, M.J. Xu, Y. Wang, B.L. Zhu, S.M. Zhang, W.P. Huang, S.H. Wu, *Cryst. Growth Des.* **9**, 3532 (2009)
19. R.W.J. Scott, S.M. Yang, G. Chabani, N. Coombs, D.E. Williams, G.A. Ozin, *Adv. Mater.* **13**, 1468 (2001)
20. C.L. Zhu, Y.J. Chen, R.X. Wang, L.J. Wang, M.S. Cao, X.L. Shi, *Sens. Actuators B* **140**, 185 (2009)